Available online at www.sciencedirect.com
ScienceDirect
Journal of Power Sources 165 (2007) 253–266
JOURNAL OF POWER SOURCES
www.elsevier.com/locate/jpowsour

A control oriented low order dynamic model for planar SOFC using minimum Gibbs free energy method☆

Handa Xi*, Jing Sun, Vasilios Tsourapas

Department of Naval Architecture and Marine Engineering, University of Michigan, Ann Arbor, MI 48109, USA

Received 21 September 2006; received in revised form 1 December 2006; accepted 5 December 2006
Available online 15 December 2006

Abstract

Given the complicated mechanisms associated with the operation of the solid oxide fuel cell (SOFC), mathematical models developed to capture the SOFC's dynamic characteristics often result in high order and complex dynamics that make the model unsuitable for control design and analysis. In this paper, the minimum Gibbs free energy (MGFE) method is exploited to simplify the calculation of the mass balance dynamics of the fuel flow in the SOFC in an effort to develop a control oriented model that achieves appropriate trade-off between model accuracy and simplicity. The simplified model is compared with a baseline model where dynamic governing equations are derived for the mass balance of each of the six gas species in the fuel flow. The implications of the MGFE method on the modeling performance are investigated through numerical simulations and frequency domain analysis. The MGFE method leads to the elimination of 5 out of 11 states in the baseline model, thereby resulting in a significantly lower order model. Critical parameters that may influence the accuracy of the simplified model are also identified. The study concludes that the accuracy of the reduced-order model is acceptable at normal conditions for both steady-state and transient operations. Noticeable model errors are only observed in steady-state responses at extreme conditions, where the fuel inlet has a high fraction of CH_4 and the fuel cell has low fuel utilization, and in transient when the inputs change at high frequency.

Keywords: Planar solid oxide fuel cell; Control-oriented dynamic model; Minimum Gibbs free energy method

1. Introduction

Given its high efficiency, low emissions and flexible fueling strategies, the solid oxide fuel cell (SOFC) offers a promising alternative energy solution for a wide range of applications. As the SOFC technology keeps evolving rapidly, dynamic mathematical models become critical tools that facilitate the design, analysis and optimization of SOFC systems. Intensified research efforts have been made on the SOFC model development in recent years, and several dynamic models have been reported [1–8]. Through model-based simulations, potential operation issues, such as the slow load following and large overshoots of the temperature and temperature gradient, have been identified in the transient response of the SOFC [8–11]. Feedback control strategies are being explored to improve the SOFC's performance [10,11].

Compared to the substantial progress achieved in the modeling, material and manufacturing of the SOFC, however, there has been much less results reported on the control design for SOFC systems in the literature. One important reason is probably because the dynamic models are often too complex for applying the model-based control methodologies. In order to capture the inherently complicated phenomena associated with the SOFC, the governing equations based on the electrochemical, thermodynamic and gas flow principles will easily drive the model to prohibitively high complexity and order. For instance, a feedback controller is designed in [11] to speed up the load following response of an SOFC system, which has 196 states in the original model. Model linearization and balanced truncation are adopted to reduce the original model down to a seven-state

Abbreviations: CPOX, catalytic partial oxidation; DIR, direct internal reforming; MGFE, minimum Gibbs free energy method; Ox, oxidation reaction; PEN, positive electrode–electrolyte–negative electrode assembly; Red, reduction reaction; SOFC, solid oxide fuel cell; SR, steam reforming; WGS, water gas shift

☆ The work reported in this paper is supported in part by the Office of Naval Research under contract N00014-06-1-0209 and in part by the Army Research Office.

* Corresponding author. Tel.: +1 734 763 7958; fax: +1 734 936 8820.
E-mail address: xih@umich.edu (H. Xi).

0378-7753/$ – see front matter © 2006 Elsevier B.V. All rights reserved.
doi:10.1016/j.jpowsour.2006.12.009

Nomenclature

A	area of the electrochemical reaction (m^2)
A_c	cross area of the gas channel (m^2)
c_p	heat capacity of solid layers ($J\,K^{-1}\,kg^{-1}$)
$c_{v,s}$	heat capacity of gaseous species s ($J\,K^{-1}\,mol^{-1}$)
C_s	molar concentration of species s ($mol\,m^{-3}$)
d	channel height (m)
e_s	specific internal energy of species s ($J\,mol^{-1}$)
F	Faraday constant ($C\,mol^{-1}$)
$h_s(T)$	specific enthalpy of species s at temperature T ($J\,mol^{-1}$)
i	current density ($A\,m^{-2}$)
$k_{f,sol}$, $k_{a,sol}$	heat transfer coefficients between bulk flows and their solid walls ($J\,K^{-1}\,m^{-2}\,s^{-1}$)
l	cell length (m)
M_s	molar mass of species s ($kg\,mol^{-1}$)
$N_{in,s}$, $N_{out,s}$	inlet and outlet molar rate of species s, respectively ($mol\,s^{-1}$)
p_s	partial pressure of gas species s (Pa)
P	total pressure (Pa)
P_0	downstream pressure of SOFC (Pa)
q_{in}, q_{out}	inlet and outlet enthalpy flux of gas flows, respectively ($J\,s^{-1}\,m^{-2}$)
r_k	rate of reaction k ($mol\,s^{-1}\,m^{-2}$)
$\tilde{R}$	universal ideal gas constant ($J\,mol^{-1}\,K^{-1}$)
T	temperature (K)
u_{out}	outlet flow velocity ($m\,s^{-1}$)
U, U_{OCV}	operating voltage and open circuit voltage of the fuel cell (V)
V	volume of gas channel (m^3)
W_{out}	outlet mass flow rate ($kg\,s^{-1}$)
X_s	molar fraction of species s

Greek symbols

α	orifice constant of gas channels (m s)
γ_{fr}	fuel utilization ratio
γ_{pr}	pre-reforming ratio
$\gamma_{O_2/C}$	oxygen-to-carbon ratio
η	potential loss (V)
$\theta_{s/C}$	molar ratio of s/C of the bulk flow in the fuel channel
$\nu_{s,k}$	stoichiometric coefficient of species s in reaction k
ρ	density ($kg\,m^{-3}$)
τ	solid layer thickness (m)

Subscripts

a	air flow
act	activation
con	concentration
f	fuel flow
I	interconnector
ohm	ohmic
Ox	oxidation reaction
PEN	PEN structure
Red	reduction reaction
s_a	species in the air flow
s_f	species in the fuel flow
sol	solid structure in SOFC
SR	steam reforming reaction
WGS	water gas shift reaction

linear one, before the linear quadratic Gaussian (LQG) method can be applied to derive feedback control laws. The disadvantages of this approach, however, include the limited applicable operating range of the resulting controller as well as the difficulty of relating the states in the reduced-order model to physical variables. In order to make the model amenable for existing control design platforms, control-oriented models, which preserve the key dynamic characteristics of the system over a wide operating range while remain low order, are in high demand to make the model-based control development possible.

One big challenge in simplifying the SOFC model attributes to the complicated composition and reactions in the bulk flow along the fuel channel. For example, while some models [2,4,6] assume that the fuel inlet to the SOFC contains only H_2 and H_2O, others [12,13] allow the carbon monoxide in the reformate entering the SOFC. In fact, CO is considered as fuel for the SOFC, either directly participating in the electrochemical reaction or producing hydrogen through the water gas shift (WGS) reaction. Direct internal reforming (DIR) is also proposed to allow hydrocarbons to be reformed directly inside the fuel channel of the SOFC [12]. Whilst these fuel flexibilities bring benefits of reducing the size of the external reformer and increasing the efficiency of the system, the complex gas compositions and chemical reactions involved lead to complicated calculations of the mass and energy balances in the SOFC. In [8], a dynamic governing equation is derived for the mass balance of each of the five species in the fuel flow, accounting for 5 out of 12 states in each discretization unit used in the finite volume method. In [1,5], the mass and energy balance in the gas flows are approximated in a quasi-static manner, resulting in a set of coupled non-linear algebraic equations that usually require extensive computational resources to solve. Although the SOFC is often modeled as a distributed parameter system, it should be noted that the issue mentioned above still exists even when the lumped parameter assumption is adopted.

The minimum Gibbs free energy (MGFE) method is an approach to obtain the equilibrium composition of chemical reactions, by minimizing the Gibbs free energy of the mixture [14]. In this paper, we use the MGFE method to simplify the calculation of the gas composition in the fuel channel and investigate the implication of this model reduction approach. For simplicity, the SOFC is considered as a lumped parameter system. A baseline model is first developed, where dynamic governing equations of mass balance are derived for each species in the fuel flow. A reduced-order model is then developed using the MGFE approach and compared to the baseline model for both

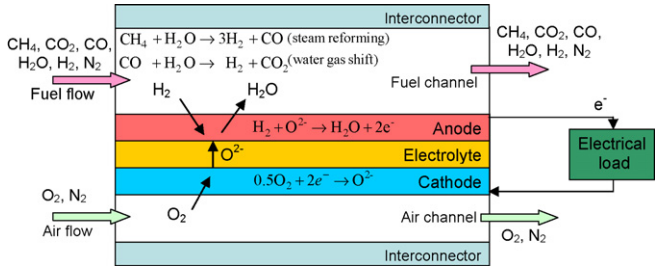

Fig. 1. Operating principle of co-flow planar SOFCs.

steady state and dynamic performance. Critical parameters that may affect the validity of the MGFE model are also identified.

The rest of the paper is organized as follows: the baseline model is described in Section 2 and a reduced-order model using the MGFE method is derived in Section 3. Based on simulation results of both steady-state and dynamic responses, these two models are then compared in Section 4, in order to investigate in depth the benefits and potential pitfalls of the simplified model. Two fuel processing methods and different operating conditions are considered in analyzing the impacts of using the MGFE method on the accuracy of the simplified model under different scenarios. Both steady-state and transient operations are considered in the analysis. The conclusions are given finally.

2. Modeling of planar SOFCs

The operating principle of the planar SOFC considered in this paper is illustrated in Fig. 1. In order to make the model compatible with different system configurations, such as different types of fuel processors and anode recirculation schemes, the fuel inlet to the fuel cell can be any combination of CH_4, CO_2, CO, H_2O, H_2 and N_2, and direct internal reforming is included in the model. Table 1 lists all the reactions to be considered in the model.

To focus on the implications of the MGFE method on model performance, the SOFC under consideration is treated as a lumped parameter system by neglecting the spatial distributions of variables, such as the current density, gas compositions, temperatures and pressures, along the direction of the bulk flows in this paper [6]. These variables are assumed to be homogeneous in the fuel cell, and the dynamic governing equations are derived by applying the electrochemical, thermal dynamic and gas flow principles. It should be noted that the proposed approach is also applicable to situations where the spatial distributions of these variables are considered. In the latter case, the system is often divided into smaller units and the governing equations can be applied to each discretization unit of the whole cell.

Table 1
Reactions considered in the model

Location	Reaction	Expression
Fuel channel	SR	$CH_4 + H_2O \rightarrow CO + 3H_2$
	WGS	$CO + H_2O \rightleftharpoons CO_2 + H_2$
Anode	Ox	$H_2 + O^{2-} \rightarrow H_2O + 2e^-$
Cathode	Red	$0.5O_2 + 2e^- \rightarrow O^{2-}$

For easier cross reference, assumptions used to develop the baseline model are summarized as follows:

(1) Current is produced only by oxidation of H_2, and CO only reacts through the WGS reaction.
(2) Ideal gas flows for both fuel and air channels.
(3) Constant Nusselt number.
(4) Adiabatic boundaries for the cell.
(5) Outlet gas flows have the same composition and temperature as inside the gas channels.

2.1. Electrochemical sub-model

The operating voltage of the cell can be calculated as follows:

$$U = U_{OCV} - (\eta_{ohm} + \eta_{act} + \eta_{con}), \quad (1)$$

where the last three terms account for various potential losses. U_{OCV} is the open circuit voltage determined by the Nernst equation:

$$U_{OCV} = E_0 - \frac{\tilde{R}T_{PEN}}{2F} \ln \frac{p_{H_2O}}{p_{H_2} p_{O_2}^{0.5}}, \quad (2)$$

with $E_0 = 1.2723 - 2.7645 \times 10^{-4} T_{PEN}$ [15], where T_{PEN} is the temperature of the PEN structure, and p_{H_2O}, p_{H_2} and p_{O_2} are the partial pressures of H_2O, H_2 and O_2, respectively.

The activation loss, η_{act}, is due to the energy barriers to be overcome in order for the electrochemical reaction to occur, and can be characterized by the Butler-Volmer equation with the transfer coefficient of 0.5 [16]. The concentration loss, η_{con}, reflects the overpotential due to the species diffusion between the reaction site and the bulk flow in gas channels, and can be calculated by the approach used in [7]. η_{ohm} is the ohmic loss due to the electrical and ionic resistance along the path of the current in the fuel cell.

2.2. Mass balance sub-model

In this sub-model, dynamic equations are derived to calculate species concentrations of the bulk flows in the fuel and air channels. The mass balance dynamics in fuel channel can be described as follows:

$$\dot{C}_{s_f} = (N_{in,s_f} - N_{out,s_f}) \frac{1}{V_f} + \sum_{k \in \{SR,WGS,Ox\}} \nu_{s_f,k} r_k \frac{1}{d_f},$$
$$s_f \in \{CH_4, CO_2, CO, H_2O, H_2, N_2\}, \quad (3)$$

where C_{s_f} is the molar concentration of species s_f in the fuel flow, N_{in,s_f} and N_{out,s_f} the inlet and outlet molar flow rates of species s_f, respectively, V_f the volume of the fuel channel, $\nu_{s_f,k}$ the stoichiometric coefficient of species s_f in reaction k, r_k the rate of reaction k, and d_f the height of the fuel channel.

According to Faraday's law, the rates of Ox and Red reactions are related to the current density as follows:

$$r_{Ox} = r_{Red} = \frac{i}{2F}. \quad (4)$$

Although different expressions are proposed to calculate the reaction rate of the SR reaction, the following formula is often used to represent the typical kinetics of the internal SR reaction in the SOFC [1,7,15–17]:

$$r_{SR} = k_{SR} p_{CH_4} \exp\left(-\frac{E_{SR}}{\tilde{R}T_f}\right), \quad (5)$$

with $k_{SR} = 0.04274\,\text{mol}\,(\text{s}\,\text{m}^2\,\text{Pa})^{-1}$ and $E_{SR} = 82,000\,\text{J}\,\text{mol}^{-1}$.

The WGS reaction is usually considered a very fast one and is assumed to be at its equilibrium [1]. The formula given in [7] is used here to account for this effect:

$$r_{WGS} = k_{WGS}\, p_{CO}\left(1 - \frac{p_{CO_2} p_{H_2}}{p_{CO} p_{H_2O} K_{eq,WGS}}\right), \quad (6)$$

where $k_{WGS} = 0.01$ in this model and $K_{eq,WGS}$ the equilibrium constant with $K_{eq,WGS} = \exp(4276/T_f - 3.961)$ [17].

While N_{in,s_f} is specified by the fuel inlet condition, N_{out,s_f} is determined by the following relation of the fuel flow continuity:

$$N_{out,s_f} = u_{out,f} C_{s_f} A_{c,f}, \quad (7)$$

where $u_{out,f}$ is the speed of the outlet fuel flow and $A_{c,f}$ the cross area of the fuel channel. Given the small pressure drop across the fuel cell, the linear orifice relation is adopted to calculate $u_{out,f}$ as follows:

$$u_{out,f} = \frac{W_{out,f}}{A_{c,f}\sum_{s_f} M_{s_f} C_{s_f}}, \quad (8)$$

$$W_{out,f} = \alpha_f (P_f - P_0), \quad (9)$$

where $W_{out,f}$ is the outlet mass flow rate of the fuel flow, M_{s_f} the molar mass of s_f, α_f the orifice constant of the fuel channel, P_f the pressure of the bulk flow in the fuel channel and P_0 is the downstream pressure of the SOFC. Plugging Eqs. (8) and (9) into Eq. (7), we have:

$$N_{out,s_f} = \frac{\alpha_f (P_f - P_0)}{\sum_{s_f} M_{s_f} C_{s_f}} C_{s_f}. \quad (10)$$

The partial pressures of species and total pressure of the fuel flow can be determined as follows:

$$p_{s_f} = \tilde{R} T_f C_{s_f}, \quad (11)$$

$$P_f = \sum_{s_f} p_{s_f}, \quad (12)$$

where T_f is the temperature of the fuel flow, which is solved in the energy balance dynamics.

Similarly, the mass balance in the air flow follows:

$$\dot{C}_{s_a} = (N_{in,s_a} - N_{out,s_a})\frac{1}{V_a} + \nu_{s_a,Red} r_{Red}\frac{1}{d_a}, \quad s_a \in \{O_2, N_2\}, \quad (13)$$

with

$$p_{s_a} = \tilde{R} T_a C_{s_a}, \quad (14)$$

$$P_a = \sum_{s_a} p_{s_a}, \quad (15)$$

$$u_{out,a} = \frac{\alpha_a (P_a - P_0)}{A_{c,a}\sum_{s_a} M_{s_a} C_{s_a}}, \quad (16)$$

$$N_{out,s_a} = u_{out,a} C_{s_a} A_{c,a} = \frac{\alpha_a (P_a - P_0)}{\sum_{s_a} M_{s_a} C_{s_a}} C_{s_a}. \quad (17)$$

2.3. Energy balance sub-model

As in [1,5], the cell is divided into three temperature layers, i.e., the fuel/air bulk flows (T_f/T_a) and solid structure (T_{sol}), where the solid structure includes both the PEN and interconnectors, i.e., $T_{PEN} = T_I = T_{sol}$. The temperatures of these layers are calculated by solving the dynamic equations of the energy balance in each layer.

The energy balance dynamics in the fuel flow can be expressed as follows:

$$\frac{d}{dt}\left(\sum_{s_f} C_{s_f} e_{s_f}\right) = (q_{in,f} - q_{out,f})\frac{1}{l} + 2k_{f,sol}(T_{sol} - T_f)\frac{1}{d_f} + r_{Ox}[h_{H_2O}(T_{PEN}) - h_{H_2}(T_f)]\frac{1}{d_f}, \quad (18)$$

where e_{s_f} is the specific internal energy of species s_f, the first term on the right hand side of Eq. (18) is due to the enthalpy flux of the bulk flow, the second term accounts for the convective heat exchange between the fuel flow and its surrounding solid layers. The heat transfer coefficient can be obtained by assuming constant Nusselt number of 4 [16]. The last term of Eq. (18) is caused by the enthalpy flux due to the Ox reaction at the anode.

By the relation for the ideal gas flow, $e_{s_f} = h_{s_f} - (p_{s_f}/C_{s_f})$, where h_{s_f} is the specific enthalpy of species s_f, we can obtain:

$$\dot{T}_f = \frac{1}{\sum_{s_f} c_{v,s_f} C_{s_f}}\left\{-\sum_{s_f}(h_{s_f}(T_f) - \tilde{R}T_f)\dot{C}_{s_f} + (q_{in,f} - q_{out,f})\frac{1}{l} + 2k_{f,sol}(T_{sol} - T_f)\frac{1}{d_f} + r_{Ox}[h_{H_2O}(T_{sol}) - h_{H_2}(T_f)]\frac{1}{d_f}\right\}, \quad (19)$$

Similarly, for the air flow, we have:

$$\dot{T}_a = \frac{1}{\sum_{s_a} c_{v,s_a} C_{s_a}}\left\{-\sum_{s_a}(h_{s_a}(T_a) - \tilde{R}T_a)\dot{C}_{s_a} + (q_{in,a} - q_{out,a})\frac{1}{l} + 2k_{a,sol}(T_{sol} - T_a)\frac{1}{d_a} - 0.5 r_{Red}\, h_{O_2}(T_a)\frac{1}{d_a}\right\}. \quad (20)$$

The inlet enthalpy flux, $q_{in,f}$ and $q_{in,a}$, are dependent upon the fuel and air inlet conditions, respectively, while the outlet enthalpy flux of the bulk flows can be calculated by:

$$q_{out,f} = u_{out,f}\sum_{s_f} C_{s_f} h_{s_f}(T_f), \quad (21)$$

$$q_{out,a} = u_{out,a}\sum_{s_a} C_{s_a} h_{s_a}(T_a). \quad (22)$$

The energy balance dynamics in the solid structure can be derived as follows:

$$\dot{T}_{\mathrm{sol}} = \frac{1}{\rho_{\mathrm{PEN}} c_{p,\mathrm{PEN}} \tau_{\mathrm{PEN}} + \rho_{\mathrm{I}} c_{p,\mathrm{I}} \tau_{\mathrm{I}}} \times \left\{ -2k_{\mathrm{f,sol}}(T_{\mathrm{sol}} - T_{\mathrm{f}}) - 2k_{\mathrm{a,sol}}(T_{\mathrm{sol}} - T_{\mathrm{a}}) + r_{\mathrm{Ox}}[h_{\mathrm{H_2}}(T_{\mathrm{f}}) + 0.5h_{\mathrm{O_2}}(T_{\mathrm{a}}) - h_{\mathrm{H_2O}}(T_{\mathrm{sol}})] - iU \right\}. \quad (23)$$

3. Model reduction for planar SOFCs using MGFE method

It is noted that the dynamic SOFC model developed in Section 2 has 11 states. Among them, six states, which represent the concentrations of the six species in the fuel flow, come from the mass balance dynamics of the bulk flow in the fuel channel. In this section, a reduced-order model is derived using the MGFE method to simplify the calculation of the composition and mass balance in the fuel flow, leading to a control-oriented SOFC model with a substantially lower order.

3.1. Composition calculation based on MGFE method

By the MGFE approach, the equilibrium composition of the chemical reactions can be obtained by minimizing the Gibbs free energy of the mixture of reactants and products [14]. Assume we consider a generic reaction as follows:

$$aA + bB \rightleftharpoons dD + eE, \quad (24)$$

and have n_s^0, $s \in \{A, B, D, E\}$ moles of species s at the beginning. Denote n_s^* as the amount of species s at the equilibrium of the above reaction at temperature T. Following the MGFE method, we have:

$$\sum_s n_s^* G_s^T = \min_{n_s} \sum_s n_s G_s^T, \quad s \in \{A, B, D, E\} \quad (25)$$

$$\text{subject to } \frac{n_{\mathrm{A}} - n_{\mathrm{A}}^0}{-a} = \frac{n_B - n_B^0}{-b} = \frac{n_D - n_D^0}{d} = \frac{n_E - n_E^0}{e} \quad (26)$$

where G_s^T is the Gibbs free energy of species s at temperature T. The constraint given in Eq. (26) follows the law of mass conservation.

The MGFE method is particularly useful when multiple chemical reactions occur simultaneously, such as the SR and WGS reactions in the fuel channel in our case. Five species, namely CH_4, CO_2, CO, H_2O and H_2, are involved in these two reactions. Since the amount of the element of carbon (C) is invariant before and after the reactions considered in the fuel channel, the MGFE method for the SOFCs fuel flow can be formulated in terms of ratios of chemical species. Define:

$$\theta_{s_0/\mathrm{C}} = \frac{N_{s_0}}{N_{\mathrm{C}}}, \quad s_0 \in \{\mathrm{C, H, O, CH_4, CO_2, CO, H_2O, H_2}\}, \quad (27)$$

where N_{s_0} is the amount (in moles) of s_0 in the fuel channel. The normalization process of Eq. (27) is beneficial, as it will reduce the number of variables that have to be considered to determine the mixture's composition.

Denote $\theta^*_{s_1/\mathrm{C}}$, $s_1 \in \{\mathrm{CH_4, CO_2, CO, H_2O, H_2}\}$ as the value of $\theta_{s_1/\mathrm{C}}$ at the equilibrium of the SR and WGS reactions. By the MGFE method, given $\theta_{\mathrm{H/C}}$, $\theta_{\mathrm{O/C}}$ and the fuel flow temperature (T_{f}), $\theta^*_{s_1/\mathrm{C}}$ satisfies:

$$\sum_{s_1} \theta^*_{s_1/\mathrm{C}} G_{s_1}^{T_{\mathrm{f}}} = \min_{\theta_{s_1/\mathrm{C}}} \sum_{s_1} \theta_{s_1/\mathrm{C}} G_{s_1}^{T_{\mathrm{f}}}, \quad s_1 \in \{\mathrm{CH_4, CO_2, CO, H_2O, H_2}\} \quad (28)$$

$$\text{subject to } \theta_{\mathrm{CH_4/C}} + \theta_{\mathrm{CO_2/C}} + \theta_{\mathrm{CO/C}} = 1,$$
$$4\theta_{\mathrm{CH_4/C}} + 2\theta_{\mathrm{H_2O/C}} + 2\theta_{\mathrm{H_2/C}} = \theta_{\mathrm{H/C}},$$
$$2\theta_{\mathrm{CO_2/C}} + \theta_{\mathrm{CO/C}} + \theta_{\mathrm{H_2O/C}} = \theta_{\mathrm{O/C}}, \quad (29)$$

where the constraints described in Eq. (29) reflect the mass conservation in terms of individual elements in the reactions.

The fuel temperature, T_{f}, can be obtained from the energy balance dynamics of the fuel flow. Considering the small volume of the fuel channel and neglecting the fuel accumulated therein, $\theta_{\mathrm{H/C}}$ and $\theta_{\mathrm{O/C}}$ in the fuel flow can be calculated by the fuel inlet condition and current density. In fact, $\theta_{\mathrm{H/C}}$ solely depends on the composition of the fuel inlet, while oxygen ions migrate from cathode to anode and enter the fuel flow through the electrochemical reactions. Define $N_{\mathrm{in,C}} = N_{\mathrm{in,CH_4}} + N_{\mathrm{in,CO_2}} + N_{\mathrm{in,CO}}$, we have:

$$\theta_{\mathrm{H/C}} = \frac{4N_{\mathrm{in,CH_4}} + 2N_{\mathrm{in,H_2O}} + 2N_{\mathrm{in,H_2}}}{N_{\mathrm{in,C}}}, \quad (30)$$

$$\theta_{\mathrm{O/C}} = \frac{2N_{\mathrm{in,CO_2}} + N_{\mathrm{in,CO}} + N_{\mathrm{in,H_2O}} + (I/2F)}{N_{\mathrm{in,C}}}. \quad (31)$$

Given the fuel inlet composition and the current drawn from the SOFC, $\theta_{\mathrm{H/C}}$ and $\theta_{\mathrm{O/C}}$ can be calculated by Eqs. (30) and (31). This allows us to represent the MGFE results for $\theta^*_{s_1/\mathrm{C}}$ as functions of only three independent variables: T_{f}, $\theta_{\mathrm{H/C}}$ and $\theta_{O/\mathrm{C}}$.

In this paper, the minimizers of Eq. (28), $\theta^*_{s_1/\mathrm{C}}$, are calculated off-line using a software named GASEQ [18], and the results are saved as look-up tables that can be used on-line in simulations. Examples of these look-up tables obtained are illustrated in Fig. 2.

Once $\theta^*_{s_1/\mathrm{C}}$ are determined, the molar fraction of individual species in the fuel channel bulk flow, denoted as $X_{s_{\mathrm{f}}}$, can be computed as follows:

$$X_{s_1} = \frac{N_{\mathrm{in,C}} \theta^*_{s_1/\mathrm{C}}}{N_{\mathrm{in,C}} \sum_{s_1} \theta^*_{s_1/\mathrm{C}} + N_{\mathrm{N_2,in}}}, \quad s_1 \in \{\mathrm{CH_4, CO_2, CO, H_2O, H_2}\}, \quad (32)$$

$$X_{\mathrm{N_2}} = \frac{N_{\mathrm{N_2,in}}}{N_{\mathrm{in,C}} \sum_{s_1} \theta^*_{s_1/\mathrm{C}} + N_{\mathrm{N_2,in}}}. \quad (33)$$

3.2. Reduced-order SOFC model using MGFE method

Instead of establishing a dynamic mass balance equation for each species in the fuel flow as been done in Section 2, we can

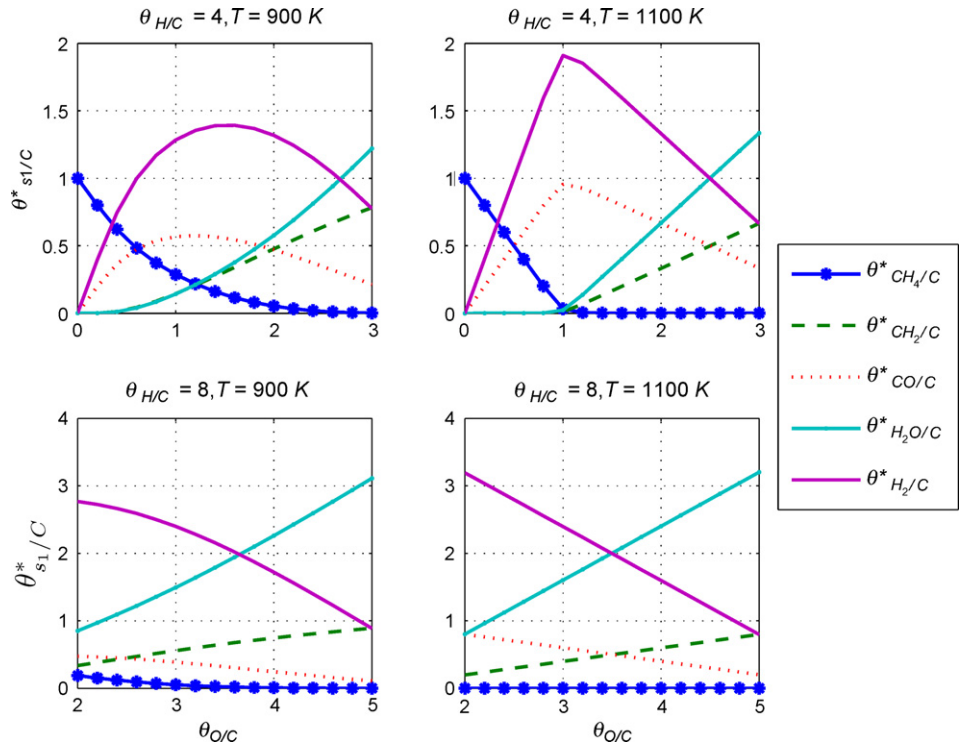

Fig. 2. Examples of look-up tables obtained by the MGFE method.

derive the following mass balance equation for the total mass of the bulk flow in the fuel channel:

$$\dot{m}_{\mathrm{f}} = W_{\mathrm{in,f}} - W_{\mathrm{out,f}} + \frac{I}{4F} M_{\mathrm{O}_2}, \tag{34}$$

where m_{f} is the total mass accumulated in the fuel channel and the last term on the right hand side accounts for the migration of the oxygen ions from the cathode to anode. From Eq. (9), we have $W_{\mathrm{out,f}} = \alpha_{\mathrm{f}}(P_{\mathrm{f}} - P_0)$ where the total pressure of the bulk flow in the fuel channel can be calculated as follows in this case:

$$P_{\mathrm{f}} = \frac{m_{\mathrm{f}}}{V_{\mathrm{f}} \sum_{s_{\mathrm{f}}} X_{s_{\mathrm{f}}} M_{s_{\mathrm{f}}}} \tilde{R} T_{\mathrm{f}}, \tag{35}$$

and consequently, the species partial pressures are $P_{s_{\mathrm{f}}} = P_{\mathrm{f}} X_{s_{\mathrm{f}}}$, where $X_{s_{\mathrm{f}}}$ is determined by Eqs. (32) and (33) based on the MGFE method.

In this paper, we focus on simplifying the mass balance in the fuel flow using the MGFE method as described above, and keep all other parts in the model given in Section 2 unchanged in order to investigate the implication of the MGFE approach. Further model simplification is possible. For example, equations similar to Eqs. (34) and (35) can also be derived for the air flow to remove one more state without having to use the MGFE approach. Furthermore, due to the small volumes of the gas channels, the mass balance and energy balance in the gas flows may be approximated in a quasi-static way to remove all the states in the mass and energy balance dynamics of the gas flows [1,5]. Given the scope of this paper, these model simplification approaches have not been applied.

For the convenience of cross reference, the model developed in Section 2 is called the baseline model and the one in this section the MGFE model in the sequel. The MGFE method leads to the elimination of five states from the fuel flow mass balance dynamics of the baseline model.

4. Model comparison

The main difference between the MGFE model and the baseline model is in the composition calculation for the fuel bulk flow. For the MGFE model, the composition is assumed to be always at the equilibrium of the SR and WGS reactions and is determined using the MGFE method. The reaction kinetics are ignored in the MGFE model but are considered in the baseline model. The WGS reaction in the SOFC is considered fast [1,5,15,16], which has been taken into account in Eq. (6). The SR reaction as described in Eq. (5), however, is a relatively slow one and may take longer time to reach its equilibrium. Therefore, prediction errors may be expected for the reduced order model derived using the MGFE approach. Impacts of the MGFE assumption on modeling results are investigated in this section by comparing the MGFE model with the baseline model through simulations and analysis.

4.1. Analysis of steady state performance

Steady-state results obtained using the MGFE and baseline models are first compared, followed by the discussion on dynamic responses in the next subsection.

Different types of fuel processors and operating conditions lead to different composition, particularly the fraction of CH_4, in the syngas fed into the fuel channel of the SOFC, which could

Table 2
Operating parameters of SOFC system

	Case number	
	1	2
Fuel processing method	SR	CPOX
Current density (i) (A cm^{-2})	0.3, 0.6	
Fuel utilization ratio (γ_{fr})	0.2, 0.4, 0.6, 0.8	
Fuel inlet temperature (K)	973	
Steam-to-carbon ratio	2	–
Pre-reforming ratio (γ_{pr})	0.2, 0.5, 0.8	–
Oxygen-to-carbon ratio ($\gamma_{O_2/C}$)	–	0.5, 0.6, 0.7
Air excess ratio	7	
Air inlet temperature (K)	973	

dictate to what extent the underlying MGFE assumption is valid. Two cases as listed in Table 2 are considered in the following, where the fuel inlet to the SOFC are the resulting reformate using two different processing methods, one with steam reforming (SR) and the other using catalytical partial oxidation (CPOX). CH_4 is used as the fuel feedstock in both cases.

4.1.1. SOFC with fuel processed by SR

In the first case, we assume that CH_4 is reformed in an external SR processor prior to the SOFC. The operating parameters of the system to be considered are listed under Case 1 in Table 2. For simplicity, the inlet temperatures of the fuel and air supplies to the SOFC, the steam-to-carbon ratio of the SR fuel processor and the air excess ratio are fixed. Different current densities (i), fuel utilization ratios (γ_{fr}) and pre-reforming ratio (γ_{pr}) are considered in simulations, where γ_{pr} is defined as follows:

$$\gamma_{pr} = \frac{\text{amount of } CH_4 \text{ reformed in the processor}}{\text{amount of } CH_4 \text{ supplied to the processor}}. \quad (36)$$

More CH_4 will remain in the reformate at lower γ_{pr}. As the DIR is possible in the SOFC, partial reformation of CH_4 in the reformer is considered and the remaining CH_4 in the reformate reacts through the DIR in the fuel channel of the SOFC.

Simulations are performed to obtain the steady-state responses of the SOFC at different operating conditions listed in Table 2. Fig. 3 compares the steady-state cell voltage and solid structure temperature (T_{sol}) predicted by the baseline model and the MGFE model. Analyzing the simulation data, one can conclude that:

(1) While the MGFE model produces significant errors at low fuel utilization ratio and low pre-reforming ratio, the two models match well at high γ_{fr} or γ_{pr}. Low fuel utilization ratios such as $\gamma_{fr} = 20\%$ lead to low SOFC efficiency

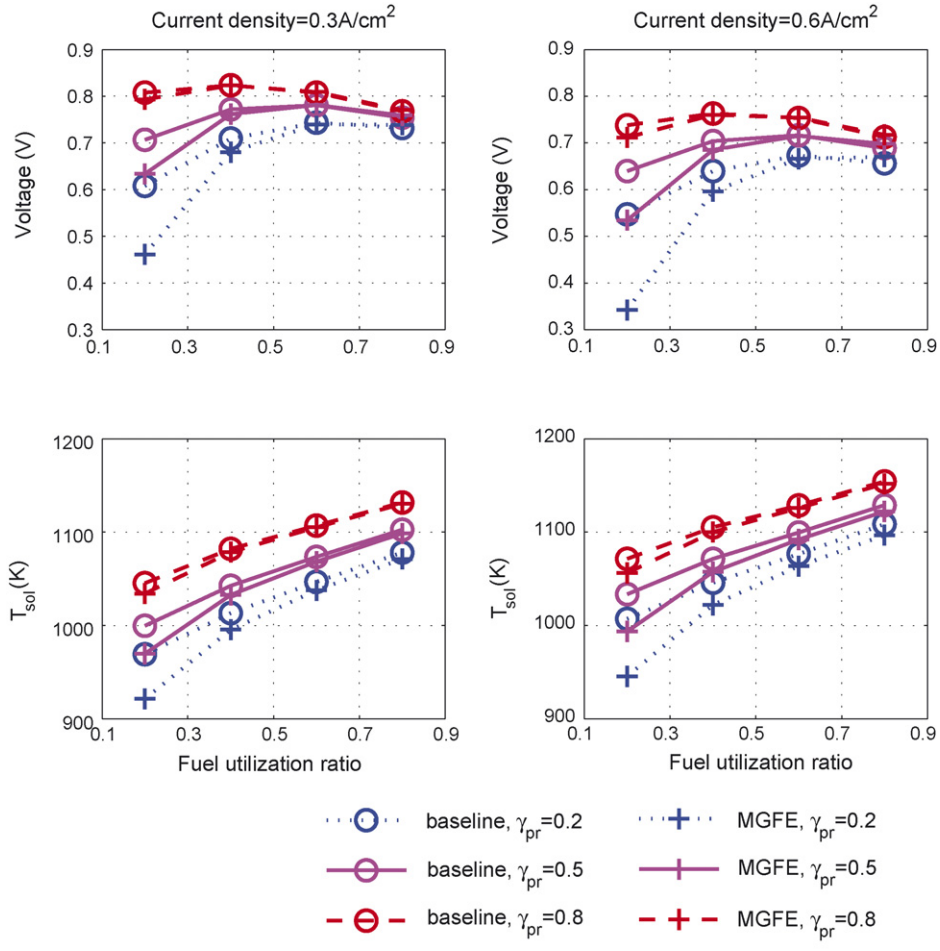

Fig. 3. Steady-state voltage and temperature of SOFC in Case 1.

Table 3
Gas composition in fuel channel of SOFC in Case 1 ($X_{N_2} = 0$)

i (A cm^{-2})	γ_{pr}	γ_{fr}	Model	X_{CH_4}	X_{CO_2}	X_{CO}	X_{H_2O}	X_{H_2}
0.3	0.8	0.8	Baseline	0.0013	0.1643	0.0348	0.6793	0.1202
			MGFE	0	0.1657	0.0343	0.6743	0.1257
		0.2	Baseline	0.0089	0.0787	0.1160	0.2967	0.4997
			MGFE	0.0005	0.0808	0.1189	0.2799	0.5199
	0.2	0.8	Baseline	0.0082	0.1697	0.0253	0.6923	0.1044
			MGFE	0	0.1700	0.0299	0.6700	0.1300
		0.2	Baseline	0.0636	0.0965	0.0654	0.3729	0.4017
			MGFE	0.0095	0.1021	0.0922	0.2744	0.5218
0.6	0.8	0.8	Baseline	0.0022	0.1630	0.0357	0.6830	0.1161
			MGFE	0	0.1642	0.0358	0.6758	0.1242
		0.2	Baseline	0.0126	0.0757	0.1167	0.3060	0.4889
			MGFE	0.0003	0.0778	0.1220	0.2826	0.5172
	0.2	0.8	Baseline	0.0126	0.1688	0.0237	0.7049	0.0901
			MGFE	0	0.1683	0.0317	0.6717	0.1283
		0.2	Baseline	0.0785	0.0917	0.0612	0.4033	0.3653
			MGFE	0.0056	0.0976	0.0990	0.2721	0.5257

and therefore are usually not expected in practical applications.

(2) T_{sol} obtained by the MGFE model is lower than that by the baseline model at all the operating conditions considered in Fig. 3, although the difference is insignificant at high γ_{fr} and γ_{pr}. The model error exhibited in T_{sol} decreases as γ_{fr} or γ_{pr} increases, while it increases as i increases.

(3) Except for γ_{fr} as high as 80%, the cell voltage predicted by the MGFE model is lower than that by the baseline model. For $\gamma_{fr} \leq 0.6$, the difference between the two models decreases as γ_{fr} increases. A decreased γ_{pr} or an increased i will lead to larger error in the steady-state cell voltage obtained by the MGFE model.

In order to further identify the root cause of the modeling error introduced by the MGFE method, the molar fractions of the gas species in the fuel channel obtained by the baseline model and the MGFE model are compared in Table 3. One can see that, under the conditions considered, the X_{CH_4} in the MGFE model is always lower than that in the baseline model, suggesting that the SR reaction be over-counted by the MGFE method, a direct result of the equilibrium assumption imposed by this approach.

Due to the strongly endothermal nature of the SR reaction, the over-counted SR reaction in the MGFE model leads to the decreased temperature in the fuel cell as shown in Fig. 3. When γ_{pr} decreases, the inlet fuel flow entering the SOFC has an increased fraction of CH_4. Therefore, the different reaction kinetics adopted in different models have more significant influence on the calculation of the fuel flow composition, leading to larger difference in X_{CH_4} and consequently in T_{sol}. This effect is exaggerated at lower γ_{fr} and higher i since the faster fuel flow involved reduces the time for CH_4 to react through the SR reaction in the fuel channel.

The cell voltage is affected by the MGFE approach primarily in two competing ways: on one hand, the decreased temperature in the SOFC will lead to reduced voltage; on the other hand, however, the high partial pressure of H_2 resulted from the increased molar fraction of H_2 in the anode due to the over-counting of the SR reaction will increase the cell voltage. The second factor is dominated by the first one in most operating conditions considered in Fig. 3. At $\gamma_{fr} = 0.8$, the second factor, however, becomes dominant where the low pressure of the hydrogen leads to the increased sensitivity of the cell voltage to the fraction of the hydrogen in the fuel channel.

4.1.2. SOFC with fuel processed by CPOX

Simulations are also performed for the case where the fuel supplied to the SOFC comes from a CPOX processor, and the operating parameters listed in the right column of Table 2 are considered. The approach used in [11] is adopted to calculate the composition of the reformate coming out of the CPOX as a function of temperature and oxygen-to-carbon ratio ($\gamma_{O_2/C}$), where $\gamma_{O_2/C}$ is defined as follows:

$$\gamma_{O_2/C} = \frac{\text{molar flow rate of } O_2 \text{ entering the reformer}}{\text{molar flow rate of } CH_4 \text{ entering the reformer}}. \quad (37)$$

Fig. 4 illustrates simulation results of the steady-state cell voltage and solid structure temperature of the SOFC at different operating conditions. No significant difference between the baseline model and the MGFE model is observed, except for the condition with γ_{fr} and $\gamma_{O_2/C}$ as low as 0.2 and 0.5, respectively. Under these conditions, the cell voltage predicted by the MGFE model is about 0.02 and 0.04 V lower than the baseline model at current density of 0.3 and 0.6 A cm^{-2}, respectively, and the solid structure temperature about 16 and 22 K lower, respectively. However, these operating conditions are not expected in real world operations, except in some short transient. For example, low $\gamma_{O_2/C}$ can lead to carbon deposition in the reformer due to low H_2O/CH_4 ratio (see Fig. 5), and therefore $\gamma_{O_2/C} \geq 0.6$ is often suggested [12]. For high system efficiency, the fuel utilization is often kept above 0.8 [19].

Similar reasons as discussed for the first case attribute to the model error introduced by the MGFE approach in this case. Table 4 compares the gas composition in the fuel channel

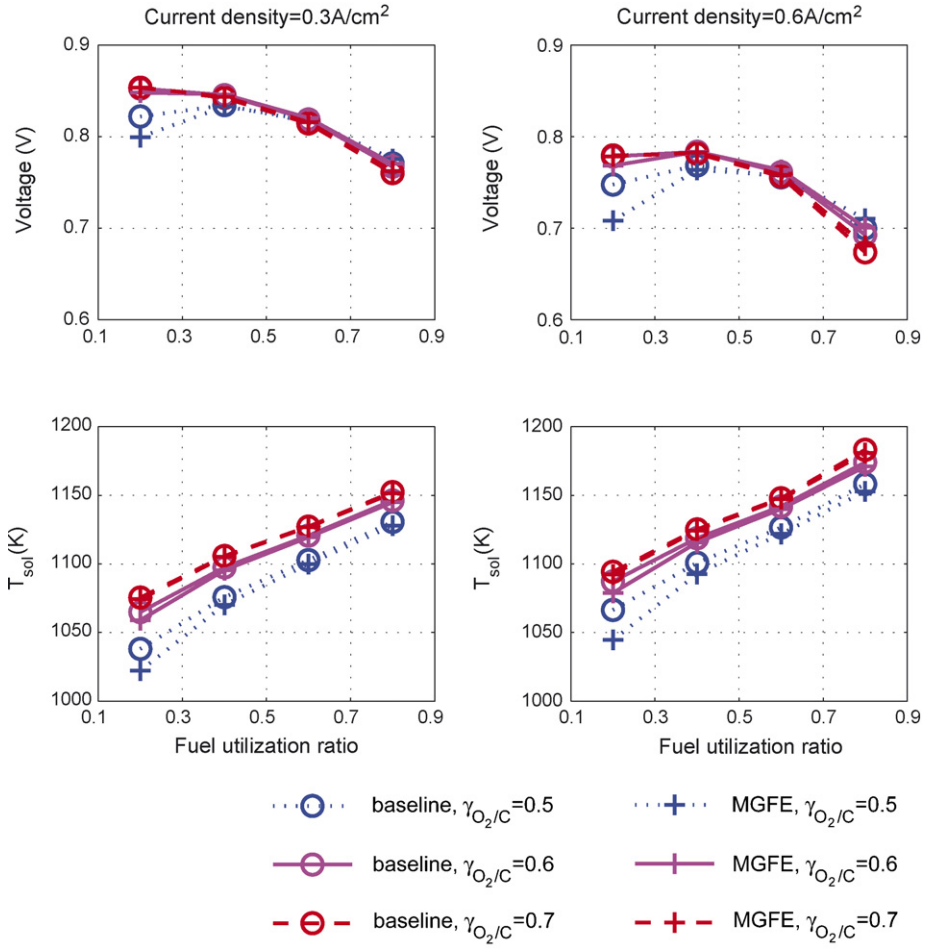

Fig. 4. Steady-state voltage and temperature of SOFC in Case 2.

obtained by the baseline model and the MGFE model. One can see that X_{CH_4} is also under-predicted by the MGFE model and the difference becomes more significant at lower γ_{fr} and $\gamma_{O_2/C}$. The molar fractions of CH_4 in the reformate fed into the fuel cell is shown in Fig. 5. As $\gamma_{O_2/C}$ decreases, more CH_4 is unreformed in the CPOX and enters the fuel channel, leading to larger error in the composition calculation in the MGFE model. The over-counted SR reaction results in the reduced temperature in the SOFC and consequently the cell voltage, as shown in Fig. 4.

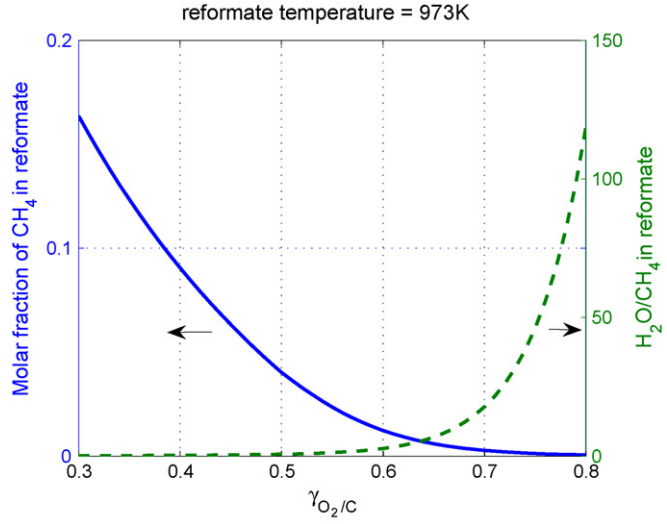

Fig. 5. Molar fraction of CH_4 and H_2O/CH_4 ratio in the reformate of CPOX.

4.2. Analysis of dynamic responses

Dynamic responses of the two models are then compared and analyzed. Given that our primary interests lie in the control system development and system integration for which the dynamic response of the system is very critical, we focus on the analysis of the model performance using both time-domain simulation and frequency domain analysis. The two cases with different fuel processing methods (i.e., SR and CPOX) are also considered here.

4.2.1. Dynamic responses of SOFC models in Case 1

Fig. 6 compares the open-loop responses of the two models in Case 1 to the step changes in the current load and gas supplies, based on simulation results. i_0 and W_{in}^0 are initial operating current density and gas inlet flow rates, respectively, corresponding to $i = 0.3\,A\,cm^{-2}$ and $\gamma_{fr} = 0.8$. Two different pre-reforming ratios ($\gamma_{pr} = 0.2, 0.8$) are considered. U_0 and T_0 are the steady-state operating voltage of the cell and the temperature in the solid

Table 4
Gas composition in fuel channel of SOFC in Case 2

i (A cm^{-2})	$\gamma_{O_2/C}$	γ_{fr}	Model	X_{CH_4}	X_{CO_2}	X_{CO}	X_{H_2O}	X_{H_2}	X_{N_2}
		0.8	Baseline	0.0005	0.1506	0.0393	0.3146	0.0652	0.4298
	0.6		MGFE	0	0.1518	0.0385	0.3124	0.0681	0.4293
		0.2	Baseline	0.0032	0.0510	0.1373	0.0977	0.2788	0.4321
0.3			MGFE	0.0003	0.0517	0.1383	0.0932	0.2868	0.4296
		0.8	Baseline	0.0016	0.1612	0.0427	0.3337	0.0741	0.3866
	0.5		MGFE	0	0.1618	0.0431	0.3300	0.0798	0.3854
		0.2	Baseline	0.0107	0.0493	0.1493	0.0869	0.3102	0.3936
			MGFE	0.0014	0.0479	0.1561	0.0767	0.3314	0.3864
		0.8	Baseline	0.0009	0.1491	0.0406	0.3166	0.0627	0.4301
	0.6		MGFE	0	0.1502	0.0400	0.3139	0.0665	0.4293
		0.2	Baseline	0.0045	0.0496	0.1378	0.1008	0.2741	0.4332
0.6			MGFE	0.0002	0.0500	0.1401	0.0948	0.2854	0.4295
		0.8	Baseline	0.0026	0.1600	0.0433	0.3368	0.0699	0.3874
	0.5		MGFE	0	0.1601	0.0448	0.3316	0.0781	0.3854
		0.2	Baseline	0.0145	0.0484	0.1480	0.0925	0.3002	0.3965
			MGFE	0.0008	0.0459	0.1585	0.0781	0.3307	0.3860

structure at the initial operating setpoints, respectively. Despite the steady-state errors as discussed earlier, the dynamic trends exhibited in the two models are more consistent, as shown in Fig. 6, even for γ_{pr} as low as 0.2.

Frequency analysis are performed to compare the dynamics of the linearized baseline and MGFE models through the bode plots as shown in Fig. 7, where two operating conditions with different γ_{pr} are considered. Frequency responses of the solid structure temperature (T_{sol}) and the cell voltage (U) to the fuel inlet flow rate ($N_{in,f}$) and the air inlet flow rate ($N_{in,a}$) are considered. Here, $N_{in,f}$ and $N_{in,a}$ are deemed as two primary inputs available for controlling the response of the SOFC. From Fig. 7, we conclude that:

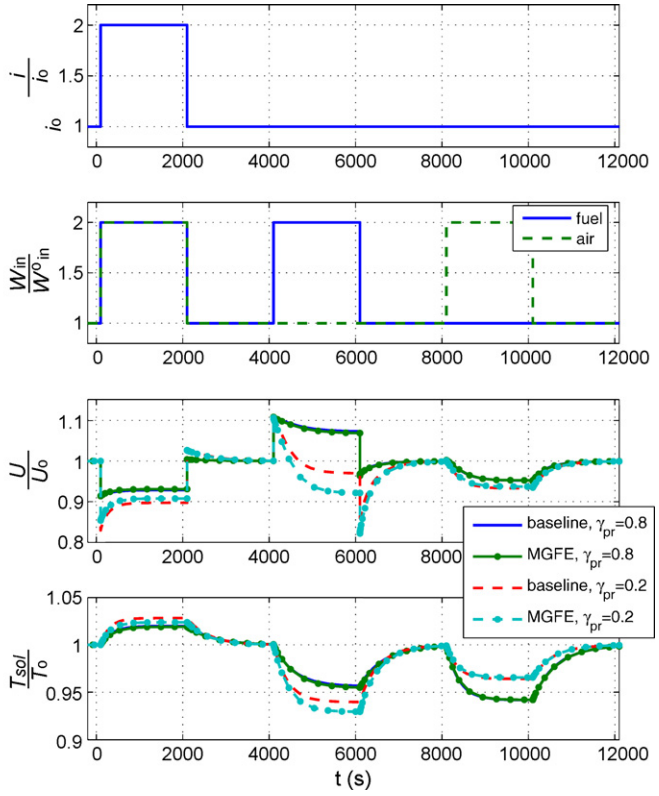

Fig. 6. Dynamic responses of the baseline and MGFE models in Case 1.

(1) Different γ_{pr} may lead to different values in gains and phases, but the correlation between the two models are similar at those two operating conditions.
(2) The MGFE model has almost the same frequency response to $N_{in,a}$ as the baseline model over a wide frequency range.
(3) The frequency responses to $N_{in,f}$ in the two models are matched well up to 0.1 rad s^{-1}, while significant model errors appear at higher frequency.
(4) The responses of T_{sol} to the inputs may be approximated by first-order dynamics for frequencies lower than 0.1 rad s^{-1}. The gains start to fall off at about 10^{-3} rad s^{-1}, which corresponds to a time constant approximately equals to 1000 s.

Since, as mentioned in Section 3, the dynamics of the air channel flow in the MGFE model are kept the same as the baseline model, it is expected that these two models have quite matched frequency response to the air flow input $N_{in,a}$, as shown in Fig. 7. For the fuel flow, however, since the mass and energy balance dynamics in the gas flows are fast, the difference in the two models as mentioned earlier results in large model errors only at high frequency, as reflected in Fig. 7. This effect is more pronounced in the response of U, compared to T_{sol}, because U can be directly affected by the gas composition in the fuel channel through the algebraic electrochemical relation.

As an illustration, Fig. 8 compares the dynamic responses of the two models to a step increase in the fuel inlet flow rate, where both short and long scope responses are shown. The simulation condition is the same as in Fig. 6 with $\gamma_{pr} = 0.8$. One can see that, while the responses of the molar fraction of H_2 and H_2O (i.e., X_{H_2} and X_{H_2O}) in the fuel channel exhibit fast dynamics in the baseline model, they change instantaneously in the MGFE model following the change in $N_{in,f}$, resulting in the instantaneous change in the cell voltage. This difference is con-

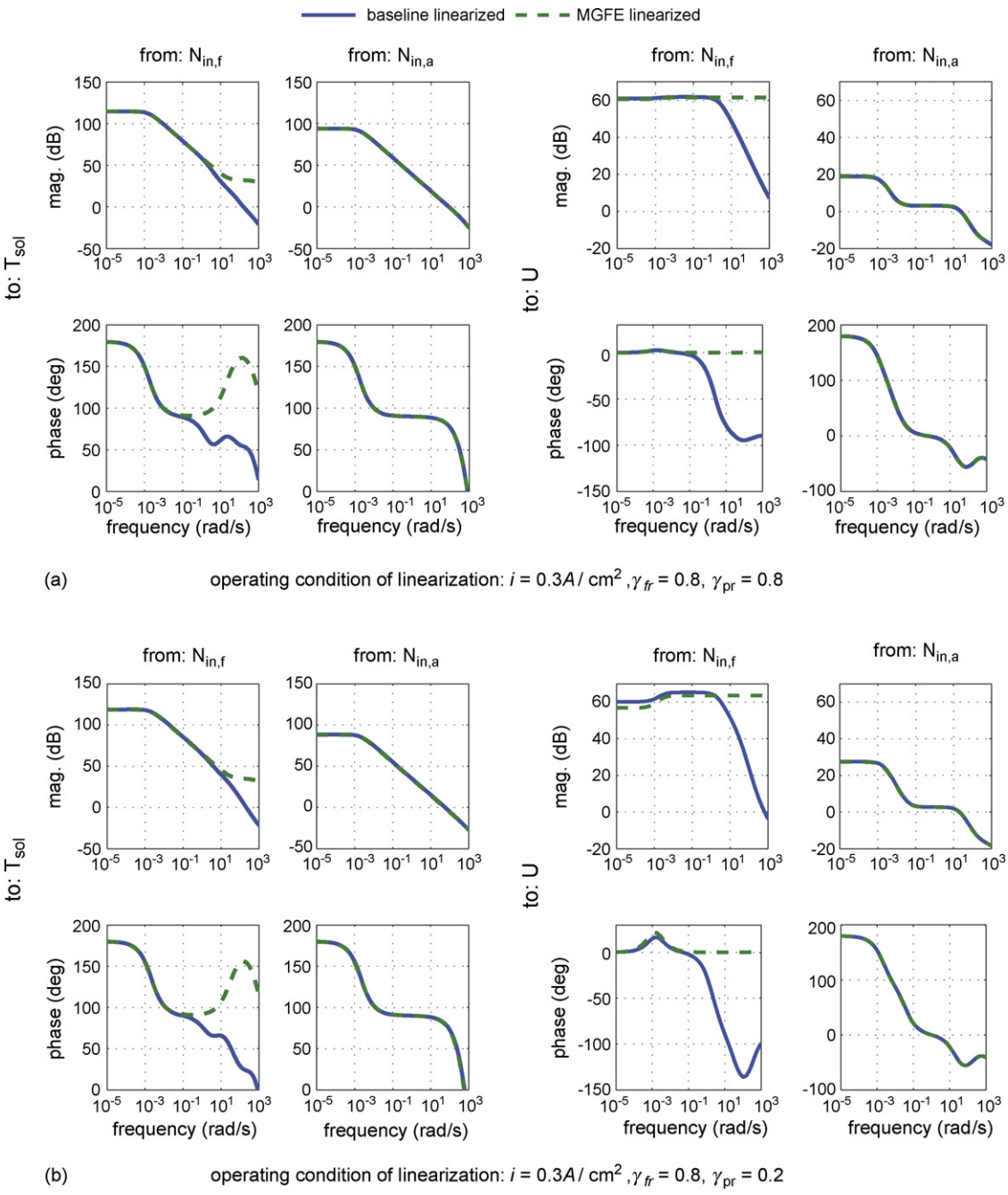

Fig. 7. Bode plots of the linearized baseline and MGFE models in Case 1.

sistent with the different dynamics between the two models at high frequency shown in Fig. 7. While the MGFE model exhibits matched behavior with the baseline model in long time horizon, it does not capture the very fast dynamics in the bulk flow in the fuel channel.

This modeling error can be mitigated by introducing a fictitious filter, which has similar characteristics as the fast dynamics shown in Fig. 8, on the input of $N_{in,f}$. Fig. 9 compares the modified MGFE model with the baseline model, where a filter with a time constant $\tau = 0.5$ s is applied to the input of $N_{in,f}$ in the MGFE model. One can see that, with this modification, the MGFE model matches the baseline model much better at high frequency, compared to the results shown in Fig. 7.

It is worth to point out that significant difference can also be found between high frequency responses of the MGFE and baseline models to the current (I) change which is considered as a disturbance input to the system in the future control design. Similar approach as mentioned above can be used to reduce the modeling error by modifying the MGFE model with simple fictitious filters.

In practical SOFC systems, since the fuel flow has to pass the fuel supply and processing subsystems, including fuel reformer, heat exchangers and gas manifolds, before reaching the fuel channel of the SOFC stack, the dynamics associated with these components will act as the filter and therefore reduce or eliminate the modeling error introduced by the MGFE assumption.

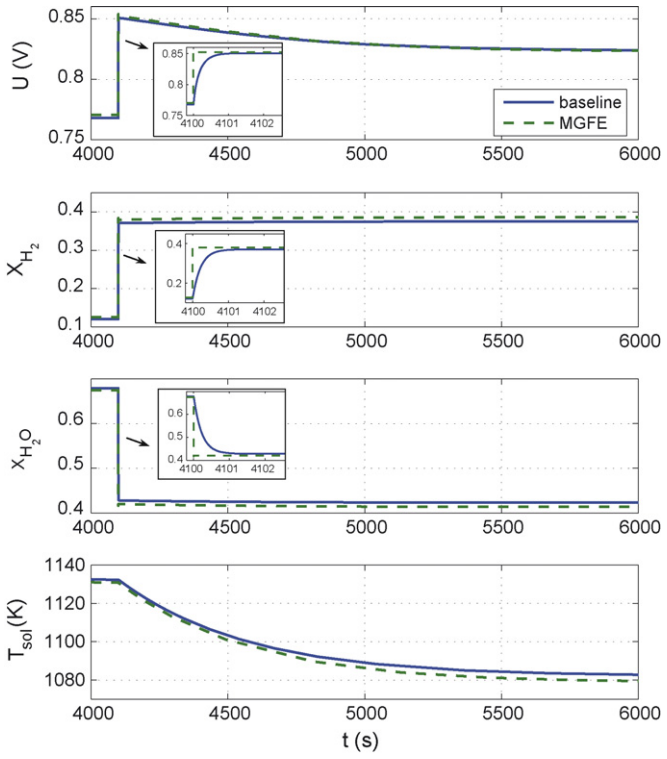

Fig. 8. Dynamic responses in short and long horizon to step increase of fuel inlet flow rate.

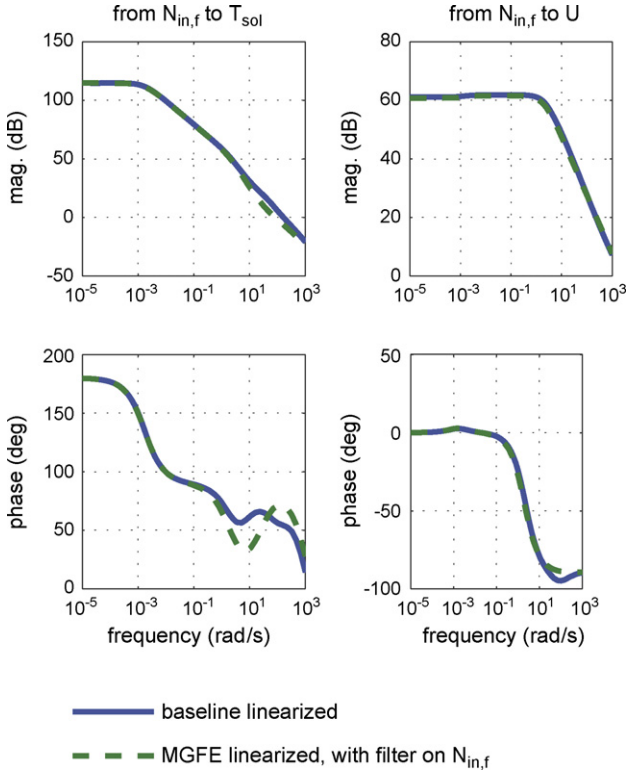

Fig. 9. Bode plots comparison with a filter $1/(0.5s+1)$ on $N_{\mathrm{in,f}}$ in MGFE model. Operating condition for linearization: Case 1, $i = 0.3\,\mathrm{A\,cm^{-2}}$, $\gamma_{\mathrm{fr}} = 0.8$ and $\gamma_{\mathrm{pr}} = 0.8$.

Besides, we are interested in the overall load following performance and the solid structure temperature in the SOFC, which are affected dominantly by the slow dynamics in T_{sol}. Therefore, given the purpose the low-order model is intended to serve, the MGFE model preserves the key dynamics in the baseline model and is amenable for model-based control design and analysis of SOFC systems.

Further inspection of Fig. 7 could also lead to the conclusion that the two inlet flow rates ($N_{\mathrm{in,f}}$ and $N_{\mathrm{in,a}}$) impart different dynamic control authorities on the system responses. While T_{sol} exhibits slow dynamics to inputs with similar time constants, the cell voltage responds differently. Two different time scales can be clearly identified: a slow one corresponding to the thermal inertia and a fast one due to the change in gas composition through mass balance dynamics. Note that $N_{\mathrm{in,f}}$ has larger gains on U compared to $N_{\mathrm{in,a}}$, suggesting it be the primary authority to control the voltage response of the SOFC. Both $N_{\mathrm{in,f}}$ and $N_{\mathrm{in,a}}$ can be used for thermal management in the cell.

4.2.2. Dynamic responses of SOFC models in Case 2

Fig. 10 compares open-loop responses of the SOFC baseline model and the MGFE model with fuel processed by a CPOX reformer (Case 2) when step changes are introduced in the current load and gas inlets. Initial operating conditions include $i = 0.3\,\mathrm{A\,cm^{-2}}$, $\gamma_{\mathrm{fr}} = 0.8$ and $\gamma_{\mathrm{O_2/C}} = 0.6/0.5$. Similar to Case 1, the dynamic responses of the simplified model match those of the baseline model. The bode plots of the linearized models in this case are also compared in Fig. 11. Similar conclusions, as elaborated in Case 1, can be drawn that the two models have close dynamic characteristics at frequency up to $0.1\,\mathrm{rad\,s^{-1}}$. While

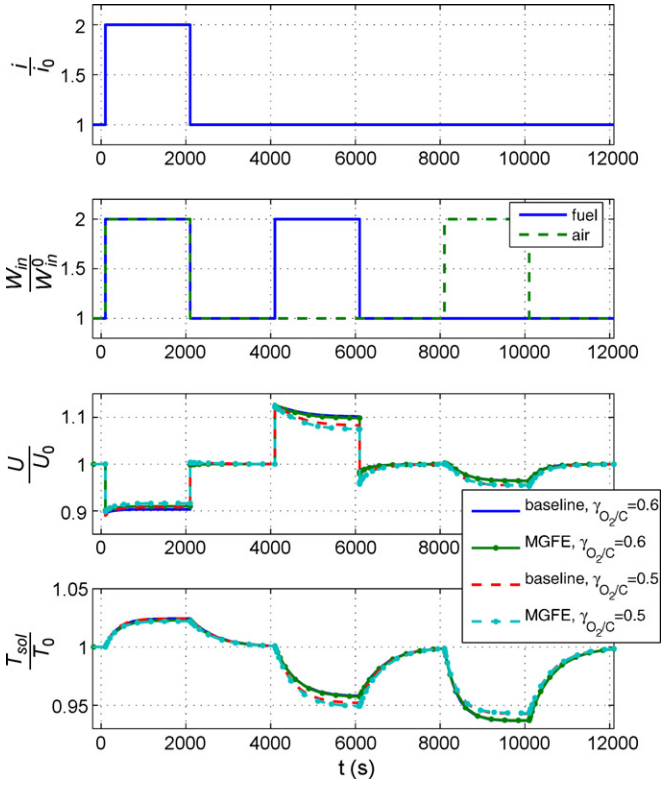

Fig. 10. Dynamic responses of the baseline and MGFE models in Case 2.

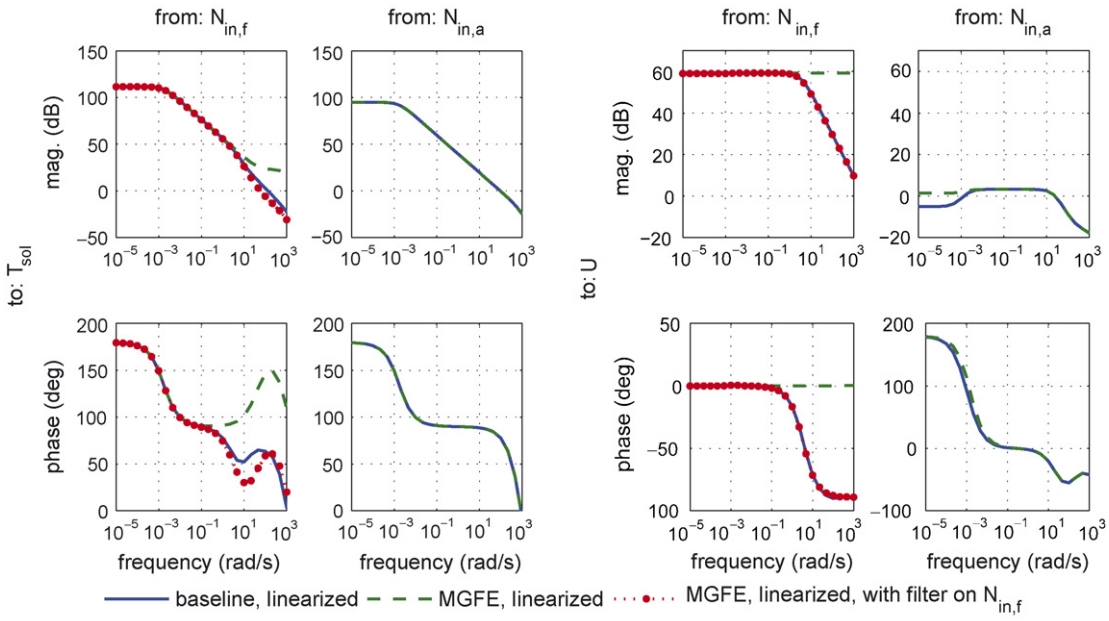

Fig. 11. Bode plots of the linearized baseline and MGFE models in Case 2 with $i = 0.3\,\mathrm{A\,cm^{-2}}$, $\gamma_{fr} = 0.8$ and $\gamma_{O_2/C} = 0.6$. Filter $= 1/(0.3s + 1)$.

Table 5
Comparison of computation efficiency

Model	Number of states in SOFC model	CPU time (s)			
		Case 1		Case 2	
		$\gamma_{pr} = 0.8$	$\gamma_{pr} = 0.2$	$\gamma_{O_2/C} = 0.6$	$\gamma_{O_2/C} = 0.5$
Baseline	11	3.14	3.26	3.80	3.24
MGFE	6	2.65	2.56	2.51	2.48

significant model errors can be found at higher frequency for the MGFE model, this error can be effectively reduced by introducing a simple filter on $N_{in,f}$ in the MGFE model. When integrated with dynamic models of fuel processing and gas supply subsystems, we can eliminate this fictitious filter as the manifold filling and other dynamics associated with the gas supply path will have the same effects.

In Table 5, computation efficiencies of the MGFE model and the baseline model are compared based on the simulation conditions for Figs. 6 and 10. The CPU time is the average of three simulations and all simulations are run on a laptop with PentiumM 1.4 GHz CPU and 512MB memory. From Table 5, it can be seen that the computation time is reduced 23.6% on average using the MGFE model, compared to the baseline model. Meanwhile, the simplified model reduce the total number of states from 11 to 6, making it more suitable for model-based control design and system optimization.

5. Conclusions

In this paper, the MGFE method is adopted to simplify the calculation of the composition and consequently the mass balance dynamics of the bulk flow in the fuel channel of the SOFC. Using this approach, 5 out of 11 states can be removed from the baseline model. Both the steady-state and dynamic responses of the simplified model and the baseline model are compared through simulations and analysis. Different compositions of the inlet fuel flow and operating conditions are considered to investigate the impacts of using the MGFE method on the modeling performance. Analysis results show that the reduced-order model is able to preserve the key dynamics exhibited by the baseline model. Good match between the two models in steady-state response is also observed at realistic operating conditions.

References

[1] E. Achenbach, J. Power Sources 49 (1994) 333–348.
[2] D. Hall, R. Colclaser, IEEE Trans. Energy Convers. 14 (3) (1999) 749–753.
[3] C. Haynes, Doctoral Thesis, Georgia Institute of Technology, USA, 1999.
[4] T. Ota, M. Koyama, C. Wen, K. Yamada, H. Takahashi, J. Power Sources 118 (2003) 430–439.
[5] L. Petruzzi, S. Cocchi, F. Fineschi, J. Power Sources 118 (2003) 96–107.
[6] K. Sedghisigarchi, A. Feliachi, J. Power Sources 149 (2005) 53–62.
[7] P. Aguiar, C. Adjiman, N. Brandon, J. Power Sources 138 (2004) 120–136.
[8] H. Xi, J. Sun, Proceedings of ASME International Mechanical Engineering Congress and Exposition, Orlando, Florida, USA, 2005.
[9] E. Achenbach, J. Power Sources 57 (1995) 105–109.
[10] P. Aguiar, C. Adjiman, N. Brandon, J. Power Sources 147 (2005) 136–147.
[11] H. Xi, J. Sun, Proceedings of ASME International Mechanical Engineering Congress and Exposition, Chicago, Illinois, USA, 2006.

[12] S. Singhal, K. Kendall (Eds.), High Temperature Solid Oxide Fuel Cells: Fundamentals, Design and Applications, Elsevier Science, 2004.
[13] J. Larminie, A. Dicks, Fuel Cell Systems Explained, 2nd ed., Wiley, 2003.
[14] W. Smith, R. Missen, Chemical Reaction Equilibrium Analysis: Theory and Algorithms, Wiley & Sons, 1982.
[15] S. Campanari, P. Iora, J. Power Sources 132 (2004) 113–126.
[16] A. Selimovic, Doctoral Thesis, Lund University, Sweden, 2002.
[17] S. Campanari, P. Iora, Fuel Cells 5 (1) (2005) 34–51.
[18] C. Morley, http://www.arcl02.dsl.pipex.com/.
[19] H. Xi, J. Sun, K. Centeck, J. King, Proceedings of Fuel Cell Seminar, 2006.